*Communication*

# One-Dimensional Organic-Inorganic Nanocomposite Synthesized with Single-Walled Carbon Nanotube Templates

**Wei Li [1],\*, Aili Wei [1], Huaiping Zhang [1] and Dojin Kim [2],\***

[1] Department of Material Science and Engineering, Taiyuan University of Technology, Taiyuan 030024, China; E-Mails: weiailidd@126.com (A.W.); huaipingzhang@gmail.com (H.Z.)

[2] Department of Material Science and Engineering, Chungnam National University, Deajeon 305764, Korea

**\*** Authors to whom correspondence should be addressed;
E-Mails: liwei03@tyut.edu.cn (W.L.); dojin@cnu.ac.kr (D.K.);
Tel.: +86-351-601-0021 (W.L.); Fax: +86-351-601-0533 (W.L.).

**Abstract:** This study reports on single-walled carbon nanotubes (SWCNT) as templates for the preparation of 1D porous organic-inorganic hybrid composites. The *in situ* deposited SWCNT were sputter coated with Sn metal and thermally oxidized in air to form a $SnO_2$/SWCNT nanowire framework on $SiO_2$/Si substrate. Poly(acrylic acid) (PAA) was coated onto this scaffold through UV light-induced radical polymerization, which resulted in the final formation of hybrid composites. The structures of hybrid composites were investigated by scanning electron microscopy, transmission electron microscopy, infrared spectroscopy, and Raman spectroscopy. The results show that PAA was successfully coated and the structural advantage of nanowire was fairly maintained, which indicates that this framework is very stable for organic functionalization in solution. The simplicity of this method for the formation of porous organic-inorganic hybrid composites provides a potential application for nanoelectronic devices.

## 1. Introduction

One-dimensional (1D) nanostructured materials have elicited significant attention because of their unique mechanical, optical, and electrical properties [1]. Template synthesis is one of the most frequent routes to synthesize 1D nanostructure. This route usually involves the use of a structure-directing reagent that facilitates the materials to adopt the desired structures [2], and thus, the premise of successful fabrication is selecting suitable template materials. Carbon nanotubes (CNTs) have been recognized as unique templates because of their structural advantages, such as their small size ranging in diameter from less than one nanometer to dozens of nanometers and extremely high length-to-diameter ratio ranging from 30 to several thousand [3]. Various 1D nanomaterials are prepared using CNT templates, but most synthesis methods are based on solution chemical methods [3–7]. These chemical methods usually suffer from poor nanostructure quality. Specifically, when transferred from solutions to substrates, these 1D nanocomposites easily aggregate due to the capillary force or van der Waals attraction, resulting in the loss of structural advantage. The situation might be changed if CNT templates have already formed a stable scaffold on substrate before mixing with solutions. According to this hypothesis, we designed a novel method to fabricate organic-inorganic nanocomposites based on CNT template.

The fabrication procedures for nanocomposites are schematically summarized in Figure 1. The synthesized single walled carbon nanotubes (SWCNTs) directly flowed onto the substrate to form a SWCNT film when the arc was discharged (Figure 1a). A thin tin metal layer was deposited over the SWCNT film by sputtering and thermally oxidized in air to form composite nanowires (Figure 1b). Finally, this $SnO_2$/SWCNT composite was further developed to form 1D organic-inorganic nanocomposite by coating a thin layer of poly(acrylic acid) (PAA) through UV light-induced radical polymerization (Figure 1c,d).

**Figure 1.** Schematic diagrams of the fabrication procedure for Poly(acrylic acid) (PAA)/$SnO_2$/single-walled carbon nanotubes (SWCNT) nanocomposites. (**a**) *In situ* deposition of SWCNT; (**b**) structural diagram of $SnO_2$/SWCNT; (**c**) diagram of UV light-induced radical polymerization of acrylic acid (AA) using benzophenone (BP) initiator; and (**d**) structural diagram of PAA/$SnO_2$/SWCNT nanocomposites.
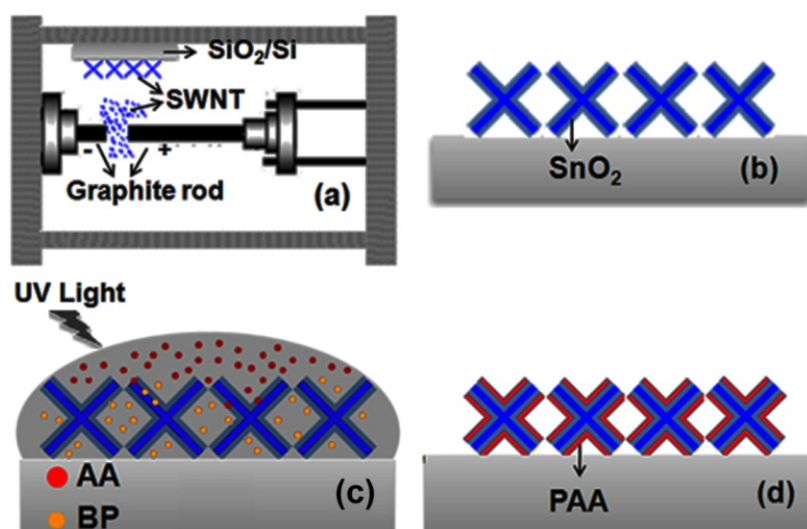
## 2. Results and Discussion

Figure 2 shows the SEM images of SWCNT template and PAA/SnO$_2$/SWCNT nanocomposite film. The SWCNTs were entangled with each other and exhibited highly porous structures (Figure 2a). The porosity of these *in situ* deposited SWCNT was estimated to be up to 95% and mainly caused by the steric hindrance effect created when the SWCNT flowed to the substrate and seat layer by layer [8]. The morphology of SnO$_2$/SWCNT is shown in Figure 2b. The shape of the composite appeared like a rope of beads instead of a regular tube-like structure, which is closely associated to the poor wetting property of SnO$_2$ on SWCNT [8]. Both SnO$_2$/SWCNT and PAA/SnO$_2$/SWCNT nanocomposites seem to duplicate structure of SWCNT template (Figure 2b,c). The SnO$_2$ deposited over SWCNT protected the morphology of SWCNT templates and ensured their application during wet chemical treatment. Notably, the extremely light SWCNT can be easily removed from the substrate. In addition, the hydrophobic nature of SWCNT can contribute to the easy collapse of their spatial structures in polar solution, such as water and methanol [9]. By contrast, PAA grafting did not significantly change the SnO$_2$/SWCNT morphology because a drop of solution contained a small amount of AA monomer. Thus, the PAAs were not sufficient to fill the pores or enclose the nanowires. The thickness of PAA/SnO2/SWCNT nanocomposite film was approximately 200 nm to 300 nm (Figure 2d).

**Figure 2.** SEM pictures of (**a**) SWCNT; (**b**) SnO$_2$/SWCNT; (**c**) PAA/SnO$_2$/SWCNT nanocomposites; and (**d**) the cross-section view of PAA/SnO$_2$/SWCNT nanocomposites.
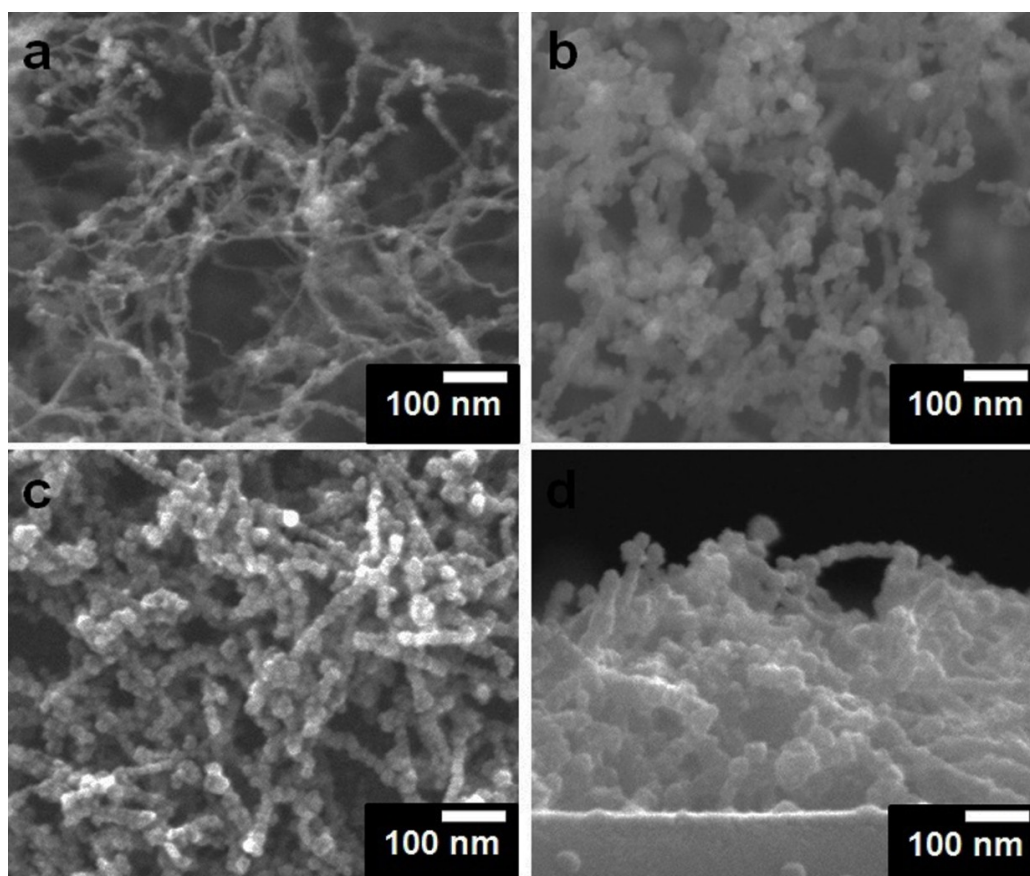


Figure 3 shows the TEM images of PAA/SnO$_2$/SWCNT nanocomposite. The SnO$_2$ beads almost completely wrapped the nanotubes, and both SWCNTs and PAA could not be clearly distinguished

under low magnification (Figure 3a). However, in a higher-resolution image (Figure 3b), PAA and a few pristine SWCNTs could be observed. The thickness of PAA coated on $SnO_2$ was from several nanometers up to 10 nm. This small thickness could not affect the integral structures, which suggests that the morphologies in SEM images did not significantly change. The inter-planar space of 0.33 nm corresponded to the (110) plane of $SnO_2$ [10].

**Figure 3.** TEM images (**a**) and its high magnification (**b**) of PAA/$SnO_2$/SWCNT nanocomposites. Inset of (**b**) shows the (110) planes of $SnO_2$.
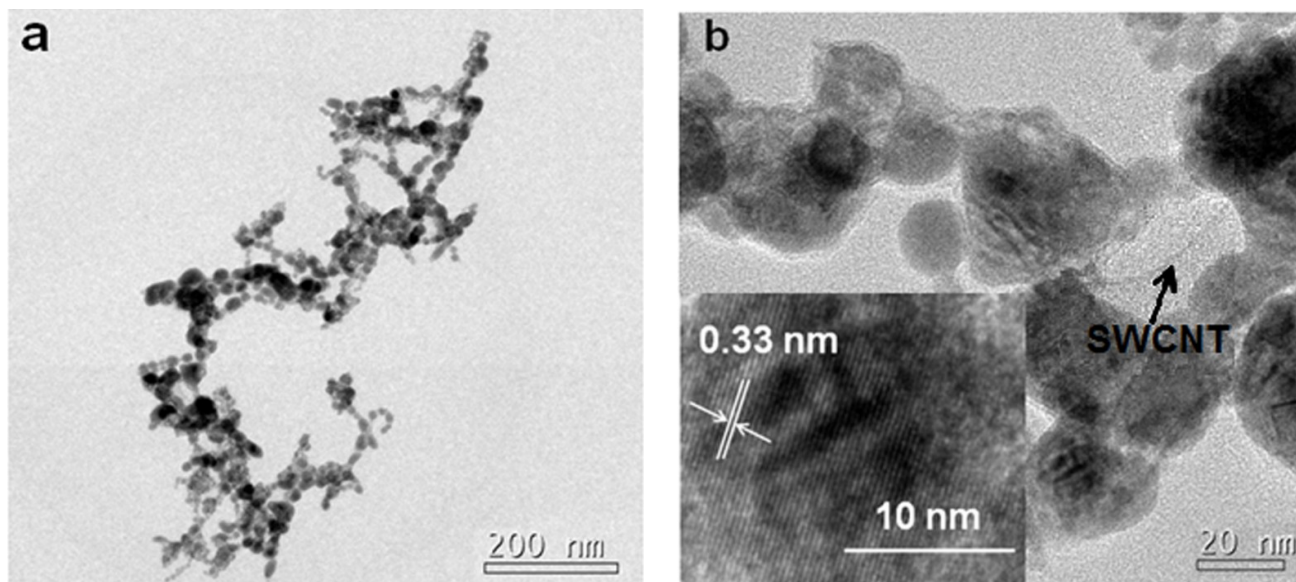


FTIR characterization is an informative approach to study the functional groups attached on $SnO_2$/SWCNTs. Figure 4 shows the FTIR spectra of nanocomposites. After coating, a group of serrate-like absorbance bands clearly appeared in the region of 1400 $cm^{-1}$ to 1800 $cm^{-1}$. The band at 1710 $cm^{-1}$ was attributed to the stretching mode of carbonyl groups, which indicates the presence of PAA on the surface of $SnO_2$/SWCNT [11]. The bands at approximately 1400 $cm^{-1}$ to 1560 $cm^{-1}$ were attributed to the stretching mode of C–O and the deformation vibration of hydroxyl. Specifically, the bands at 1408 and 1545 $cm^{-1}$ were due to the binding of the carboxylic acid groups to the surface of $SnO_2$ nanobeads to form carboxylate groups [12].

Raman spectra as complementary investigation to FTIR are shown in Figure 5. Two distinct peaks associated to the vibration modes of SWCNTs within the region of 1200 $cm^{-1}$ to 1800 $cm^{-1}$ were observed [13]. The peak at 1590 $cm^{-1}$, the so-called G band, corresponded to the $sp_2$ vibration of a 2D hexagonal lattice in the graphite; another peak at 1350 $cm^{-1}$, the so-called D band, was associated to glassy carbon or disordered graphite. The intensity of D band significantly increased and the corresponding G band intensity decreased in the spectrum of nanocomposite. In general, the intensity ratio of D to G band is a sign of defect/amorphous carbon concentration in SWCNTs [14]. The D/G intensity ratio of 1.03 for nanocomposite was much higher than that of 0.18 for SWCNTs, which indicates that PAA/$SnO_2$ coating created more defects on the SWCNT surface. In addition, the radial breathing mode (RBM) in the range of 100–300 $cm^{-1}$ was present in spectrum of SWCNT, and the tube diameters were approximately 1.4 nm from the RBM frequency [8,15,16]. Furthermore, no RBM signal was present in the spectrum of nano-composite. The possible reason is that PAA/$SnO_2$ coating

increases the thickness and surface defect of SWCNT bundles, resulting in a reducing of signal [17]. Three bands of $SnO_2$ at 304, 614, and 670 $cm^{-1}$ were observed in the nanocomposite spectrum. The band at 304 $cm^{-1}$ corresponded to the infrared-active $E_u$ (TO) mode [18,19], and the band at 614 $cm^{-1}$ was associated with the Raman-active $A_{1g}$ mode [18]. The band at 670 $cm^{-1}$ possibly indicated other tin oxide stoichiometries [20].

**Figure 4.** FTIR spectra of (**a**) $SnO_2$/SWCNT and (**b**) PAA/$SnO_2$/SWCNT nanocomposites.
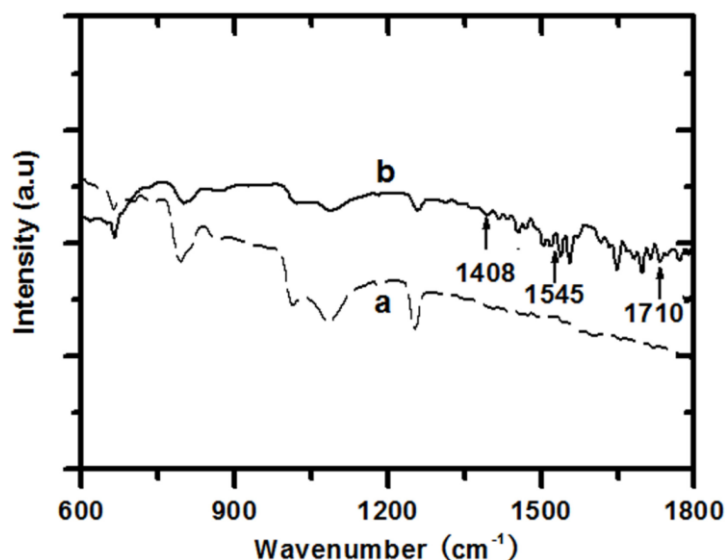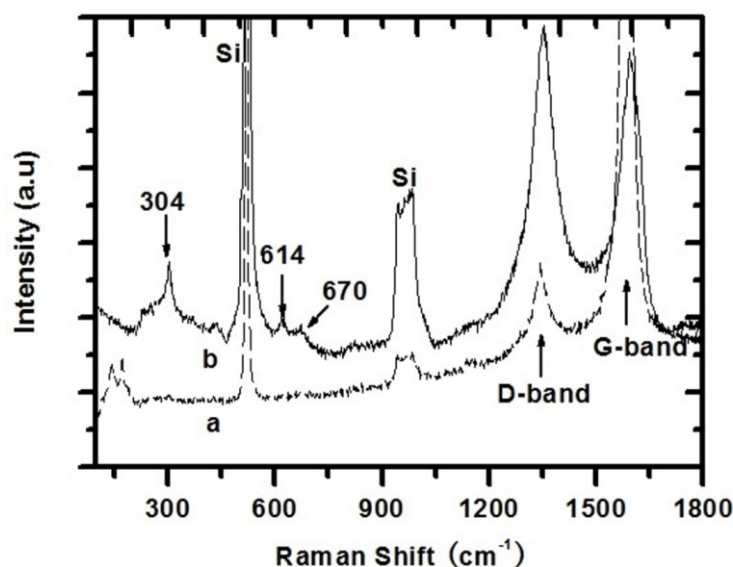


**Figure 5.** Raman spectra of (**a**) SWCNT and (**b**) PAA/$SnO_2$/SWCNT nanocomposites.



Raman mode bands at approximately 520 and 950 $cm^{-1}$ in both spectra were associated with the vibration mode of the substrate. Their appearances were due to the high film porosity, which allowed the laser beam to penetrate down to the substrate. Meanwhile, their intensities in the nanocomposite were much higher than those in SWCNTs. This phenomenon was possibly associated with the film thickness because PAA and $SnO_2$ coating will reduce the overall film thickness and allow the laser beam to penetrate more easily. Furthermore, no characteristic peaks of PAA were observed [21–23]; they probably overlapped with the strong substrate peaks.

## 3. Experimental Section

### 3.1. Synthesis of SnO₂/SWCNT

The $SiO_2$/Si substrates were mounted on the wall of an arc-discharging chamber. When the arc was discharged, the synthesized SWCNT directly flowed onto the substrate and formed a film. The source material for arc discharge was a graphite rod where catalytic metal wires of Ni, Fe, and Mo were inserted. The synthesis was carried out in an optimized condition with an arc current density of 80 A/cm$^2$ in H$_2$ atmosphere at 400 Torr for 1 min [13]. The SWCNT film was first installed in a sputtering chamber equipped with a tin target. The tin was deposited in Ar gas atmosphere at room temperature and heated in a tube furnace in air (450 °C) for 2 h to form $SnO_2$/SWCNT composite nanowires.

### 3.2. Synthesis of PAA/SnO₂/SWCNT Composite

AA monomer and benzophenone (BP) initiator were purchased from Sigma-Aldrich (Shanghai, China) and used without further purification. The $SiO_2$/Si substrate covered by $SnO_2$/SWCNT composite nanowires was immersed in BP methanol solution for 20 min and dried for 2 h at room temperature to deposit the BP molecules onto the nanowire surface. A drop of AA solution (5 wt%) was placed on the substrate, and then the substrate was enclosed in a photo-reactor and irradiated by UV light at room temperature. Finally, the nanocomposite film was washed with distilled water and methanol to eliminate the residual monomer, BP initiator, and homopolymer.

### 3.3. Characterizations

Scanning electron microscopy (SEM) measurements were obtained using a JEOL-7000 instrument (Tokyo, Japan) at an accelerating voltage of 15 kV. Transmission electron microscopy (TEM) measurements were carried out using a FEI Tecnai F30 instrument (Eindhoven, The Netherlands) at an accelerating voltage of up to 200 kV. The samples were placed on 300 mesh carbon-coated copper grid. Fourier transform infrared (FTIR) spectroscopy was recorded using a Bio-Rad FTS-175C instrument (Hercules, CA, USA). Raman spectroscopy measurements were recorded in backscattering geometry with a Horiba LabRam HR instrument fitted with a liquid nitrogen-cooled CCD detector (Paris, France). The spectra were collected under ambient conditions using the 514.5 nm line of an argon-ion laser.

## 4. Conclusions

In summary, the PAA was successfully coated onto the surface of $SnO_2$/SWCNT nanowires and formed 1D PAA/$SnO_2$/SWCNT nanocomposites through UV light-induced radical polymerization. The nanocomposite not only had a chemical affinity property of PAA but also essentially maintained the structural property of SWCNT templates, confirming that the method used in this work is very suitable to prepare a stable 1D template for organic functionalization in solution. In further studies, we will not only focus on the application of PAA/$SnO_2$/SWCNT nanocomposite to nanoelectrical devices, such as gas sensors and glucose biosensors, but also utilize this method to make other hybrid nanocomposites, such as polyaniline/$SnO_2$/SWCNT.

## Acknowledgments

## Conflicts of Interest

The authors declare no conflict of interest.

## Author Contributions

Wei Li and Dojin Kim designed the study, performed the experiments, and analyzed the data. Wei Li, Aili Wei, and Huaiping Zhang wrote the paper.

## References

1. Penner, P.M. Chemical sensing with nanowires. *Annu. Rev. Anal. Chem.* **2012**, *5*, 461–485.
2. Doménech-Carbó, A. *Electrochemistry of Porous Materials*, 1st ed.; CRC Press: London, UK, 2010; p. 5.
3. Tessonnier, J.P.; Winé, G.E.; Leuvery, C.; Ledoux, M.J.; Pham-Huu, C. Carbon nanotube as 1D templates for the synthesis of air sensitive materials: About the confinement effect. *Catal. Today* **2009**, *102–103*, 29–33.
4. Ding, S.; Li, C.; Lei, W.; Zhang, Y.; Qasim, K.; Cui, H.; Zhang, X.; Wang, B. Stable and uniform field emission from zinc oxide nanowires grown on carbon nanotube mesh template. *Thin Solid Films* **2012**, *524*, 245–248.
5. Pint, C.L.; Nicolas, N.W.; Xu, S.; Sun, Z.; Tour, J.M.; Schmidt, H.K.; Gordon, R.G.; Hauge, R.H. Three dimensional solid state supercapacitors from aligned single walled carbon nanotube array templates. *Carbon* **2011**, *49*, 4890–4897.
6. Peng, H.; Sun, X. Macroporous carbon nanotube arrays with tunable pore sizesand their template applications. *Chem. Commun.* **2009**, *45*, 1058–1060.
7. Yang, H.; Zhang, D.; Shi, L.; Fang, J. Synthesis and strong red photoluminescence of europium oxide nanotubes and nanowires using carbon nanotubes as templates. *Acta Mater.* **2008**, *56*, 955–967.
8. Nguyen, D.H.; Nguyen, V.Q.; Song, H.; Kang, Y.; Cho, Y.; Kim, D. Tin oxidenanotube structures synthesized on a template of single-walled carbon nanotubes. *J. Cryst. Growth* **2009**, *311*, 657–661.
9. Nguyen, D.H.; Nguyen, V.Q.; Cho, Y.; Kim, D. Porous Single-wall carbon nanotube films formed by *in situ* acr discharge deposition for gas sensors application. *Sens. Actuators B Chem.* **2009**, *135*, 656–663.
10. Zhou, Z.; Wu, J.; Li, H.; Wang, Z. Field emission from *in situ* grown vertically aligned $SnO_2$ nanowire arrays. *Nanoscale Res. Lett.* **2012**, *7*, 117–123.
11. Chen, S.; Wu, G.; Liu, Y.; Long, D. Preparation of poly(acrylic acid) grafted multiwalled carbon nanotube by a two step irradiation technique. *Macromolecules* **2006**, *39*, 330–334.
12. Lin, C.L.; Lee, C.F.; Chiu, W.Y. Preparation and properties of poly(acrylic acid) oligomer stabilized superparamagnetic ferrofluid. *J. Colloid Interface Sci.* **2005**, *291*, 411–420.

13. Li, W.; Jung, H.; Nguyen, D.H.; Kim, D.; Hong, S.K.; Kim, H. Nnaocomposite of cobalt oxide nanocrystals and single-walled carbon nanotubes for a gas sensor application. *Sens. Actuators B Chem.* **2010**, *150*, 160–166.

14. Silambarasan, D.; Surya, V.J.; Vasu, V.; Iyakutti, K. Investigation of single-walled carbon nanotubes titanium metal composite as a possible hydrogen storage medium. *Int. J. Hydrog. Energy* **2013**, *38*, 14654–14660.

15. García-Gutiérrez, M.C.; Nogales, A.; Rueda, D.R.; Domingo, C.; García-Ramos, J.V.; Broza, G.; Roslaniec, Z.; Schulte, K.; Davies, R.J.; Ezquerra, T.A.; *et al.* Templating of crystallization and shear induced self-assembly of single-wall carbon nanotubes in a polymer-nanocomposite. *Polymer* **2006**, *47*, 341–345.

16. Bandow, S.; Asaka, S.; Saito, Y.; Rao, A.M.; Grigorian, L.; Richter, E.; Eklund, P.C. Effect of the growth temperature on the diameter distribution and chirality of single-wall carbon nanotubes. *Phys. Rev. Lett.* **1998**, *80*, 3779–3782.

17. Coata, S.; Borowiak-Palen, E. Diameter sensitive effect in single walled carbon nanotubes upon acid treatment. *J. Alloys Compd.* **2009**, *486*, 386–390.

18. Sun, S.H.; Meng, G.W.; Zhang, G.X.; Gao, T.; Geng, B.Y.; Zhang, L.D.; Zuo, J. Raman scattering study of rutile $SnO_2$ nanobelts synthesized by thermal evaporation of Sn powders. *Chem. Phys. Lett.* **2003**, *376*, 103–107.

19. Cheng, G.; Wang, J.; Liu, X.; Huang, K. Self-assembly synthesis of single crystalline tin oxide nanostrucutres by a poly(acrylic acid)-assisted solvothermal process. *J. Phys. Chem. B* **2006**, *110*, 16208–16211.

20. Liu, L.Z.; Li, T.H.; Wu, X.L.; Shen, J.C.; Chu, P.K. Identification of oxygen vacancy types from Raman spectra of $SnO_2$ nanocrystals. *J. Raman Spectrosc.* **2012**, *43*, 1423–1426.

21. Murli, C.; Song, Y. Pressure-induced polymerization of acrylic acid: A raman spectroscopic study. *J. Phys. Chem. B* **2010**, *114*, 9744–9750.

22. Todica, M.; Dinte, E.; Pop, C.V.; Farcau, C.; Astilean, S. Raman investigation of some polymeric gels of pharmaceutical interest. *J. Optoelectron. Adv. Mater.* **2008**, *10*, 823–825.

23. Dong, J.; Ozaki, Y.; Nakashima, K. Infrared, Raman, and near-infrared spectroscopic evidence for the coexistence of virous hydrogen-bond forms in poly(acrylic acid). *Macromolecules* **1997**, *30*, 1111–1117.